10-1-2014

A transgenic zebrafish model expressing KIT-D816V recapitulates features of aggressive systemic mastocytosis

Tugce B. Balci
IWK Health Centre, tugce.balci@lhsc.on.ca

Sergey V. Prykhozhij
IWK Health Centre

Evelyn M. Teh
IWK Health Centre

Sahar I. Da'as
IWK Health Centre

Eileen Mcbride
IWK Health Centre

See next page for additional authors

bjh research paper

A transgenic zebrafish model expressing *KIT*-D816V recapitulates features of aggressive systemic mastocytosis

Tugce B. Balci,[1,2]* Sergey V. Prykhozhij,[1]* Evelyn M. Teh,[1] Sahar I. Da'as,[1] Eileen McBride,[1,3] Robert Liwski,[4] Ian C. Chute,[5] Daniel Leger,[5] Stephen M. Lewis[5,6,7,8] and Jason N. Berman[1,4,6,9]

[1]Department of Pediatrics, IWK Health Centre, Halifax, NS, [2]Department of Medical Genetics, University of Ottawa, [3]Department of Pediatrics, Montfort Hospital, Ottawa, ON, [4]Department of Pathology, Dalhousie University, Halifax, NS, [5]Atlantic Cancer Research Institute, Moncton, NB, [6]Department of Microbiology & Immunology, Dalhousie University, Halifax, NS, [7]Department of Biology, University of New Brunswick (Saint John), Saint John, [8]Department of Chemistry & Biochemistry, Université de Moncton, Moncton, NB, and [9]Department of Pediatrics, Dalhousie University, Halifax, NS, Canada

Received 2 March 2014; accepted for publication 20 May 2014

Correspondence: Jason N. Berman, IWK Health Centre, PO Box 9700, 5850/5980 University Avenue, Halifax, NS B3K 6R8, Canada.
E-mail: jason.berman@iwk.nshealth.ca
*These authors contributed equally to this work.

Summary

Systemic mastocytosis (SM) is a rare myeloproliferative disease without curative therapy. Despite clinical variability, the majority of patients harbour a *KIT*-D816V mutation, but efforts to inhibit mutant KIT with tyrosine kinase inhibitors have been unsatisfactory, indicating a need for new preclinical approaches to identify alternative targets and novel therapies in this disease. Murine models to date have been limited and do not fully recapitulate the most aggressive forms of SM. We describe the generation of a transgenic zebrafish model expressing the human *KIT*-D816V mutation. Adult fish demonstrate a myeloproliferative disease phenotype, including features of aggressive SM in haematopoeitic tissues and high expression levels of endopeptidases, consistent with SM patients. Transgenic embryos demonstrate a cell-cycle phenotype with corresponding expression changes in genes associated with DNA maintenance and repair, such as reduced *dnmt1*. In addition, *epcam* was consistently downregulated in both transgenic adults and embryos. Decreased embryonic *epcam* expression was associated with reduced neuromast numbers, providing a robust *in vivo* phenotypic readout for chemical screening in *KIT*-D816V-induced disease. This study represents the first zebrafish model of a mast cell disease with an aggressive adult phenotype and embryonic markers that could be exploited to screen for novel agents in SM.

Keywords: zebrafish, systemic mastocytosis, transgenesis, *KIT* D816V, receptor tyrosine kinase.

Mast cells are well known to play critical roles in both innate and adaptive immune responses, as well as allergic reactions and inflammation (Theoharides & Kalogeromitros, 2006; Metcalfe, 2008). Similarly, mast cells have been implicated in autoimmune conditions (Metcalfe, 2008) and neoplastic processes (Ribatti *et al*, 2004, 2009). The elucidation of the various functions of mast cells has been largely due to the characterization of their receptors, KIT and FCεRI, and their respective signal transduction pathways responsible for growth, differentiation, survival and physiological functions (Metcalfe, 2008). Perturbed mast cell development and proliferation results in a pathological accumulation of mast cells, known as mastocytosis and classified among the myeloproliferative disorders (Robyn & Metcalfe, 2006; Takemoto *et al*, 2009). The clinical spectrum of systemic mastocytosis (SM) encompasses a wide range of clinical presentations, from a localized skin disease to an aggressive leukaemia (Metcalfe & Akin, 2001; Patnaik *et al*, 2007; Pardanani, 2012). Most patients harbour a common point mutation in the *KIT* gene, namely the Asp816Val (D816V) substitution. KIT is a transmembrane receptor with intrinsic tyrosine kinase activity found on many types of haematopoietic cells, however, only mast cells retain high levels of *KIT* expression in their mature form, while others gradually lose *KIT* expression after the progenitor stage (Metcalfe, 2008). This mutation leads to pathological constitutive phosphorylation of the KIT receptor, resulting in activation of downstream effectors, such as Ras/Raf/MAPK and JAK/STAT pathways, that lead to

First published online 2 July 2014
doi: 10.1111/bjh.12999

increased mast cell migration and survival and contribute to disease pathogenesis (Nagata *et al*, 1995; Longley *et al*, 1996; Metcalfe & Akin, 2001; Pardanani, 2012). Despite this specific defect leading to activation of a protein kinase receptor, to date there is no effective targeted therapy available for SM. Moreover, the same *KIT*-D816V mutation is present across the spectrum of SM phenotypes, indicating that additional genetic lesions and/or activation of parallel pathways collaborate to induce a more aggressive disease. Current treatment is tailored to patient symptoms and management in advanced disease is not standardized (Metcalfe, 2008; Pardanani, 2012). Pertinent animal models of SM are necessary preclinical tools to elucidate contributing molecular pathways in disease pathogenesis and as a platform for *in vivo* screening of novel therapeutics.

Mouse models of SM created by employing different approaches have been published. Zappulla *et al* (2005) used the primate chymase promoter to drive the human *KIT*-D816V mutation and observed a spontaneous accumulation of mast cells in tissues and at least one mast cell tumour in 30% of adult transgenic animals. More recently, Gerbaulet *et al* (2011) described mast cell hyperplasia, B-lymphocyte neoplasia and colitis in their inducible Cre/loxP-based transgenic mouse model, where they overexpressed the murine homolog of the human *KIT*-D816V mutation, *Kit*-D814V. While providing valuable insight into the transforming capabilities of KIT and mastocytosis-like findings, this model was associated with a 75% perinatal lethality of transgenic animals. The phenotypes observed revealed the pleiotropic effects of mutant KIT, but limited the possibility of studying the effects of the mutation into adulthood.

In the last two decades, the zebrafish (*Danio rerio*) has emerged as a powerful tool for modelling human diseases, due to its many advantages as an experimental vertebrate. Highly conserved genetics together with advancements in transgenic technology and traceable development in externally developing transparent embryos have enabled the successful establishment of an increasing number of human disease models (Langenau *et al*, 2003; Patton *et al*, 2005; Santoriello *et al*, 2010; Chen & Langenau, 2011). Furthermore, the ease and availability of genetic manipulation and unprecedented live imaging capabilities have provided valuable insight into vertebrate haematopoietic and immunological development and cell function (Berman *et al*, 2003; Traver *et al*, 2003; Martin & Feng, 2009; Jing & Zon, 2011; Yoo *et al*, 2011; Renshaw & Trede, 2012).The zebrafish also has an inherent capacity to accommodate high-throughput chemical modifier screens, which have previously identified effective compounds in a variety of disease states in zebrafish models (Peterson *et al*, 2000; Burns *et al*, 2005; North *et al*, 2007; Yeh *et al*, 2009; Tsang, 2010). We employed these opportunities to identify mast cells and a specific lineage marker (*carboxypeptidase A5*) in the zebrafish (Dobson *et al*, 2008); demonstrate structural and functional conservation of these cells (Da'as *et al*, 2011) and, more recently, elucidate the role of Notch signalling in the transcriptional regulation of mast cell lineage commitment (Da'as *et al*, 2012). Given this conservation of mast cell biological processes, we wanted to exploit the advantages of the zebrafish system to study hyperproliferative mast cell diseases. Here we describe a transgenic zebrafish model of SM generated using the human *KIT*-D816V mutation that exhibits a mast cell proliferative phenotype in adult fish and results in changes in specific embryonic markers, providing a new *in vivo* tool for future experiments and drug screening in this disease model. The overall importance of the zebrafish model of SM lies in additional experimental opportunities for studies of this disease that may not be available in other model systems.

Methods

Zebrafish husbandry and maintenance

Zebrafish husbandry was carried out according to standard protocols (Westerfield, 2007). The use of zebrafish in these studies has been approved by the Dalhousie University Committee on Laboratory Animals, under protocol number 11–128. Embryos lacking pigmentation were obtained through incubation in embryo media containing 0·003% N-phenylthiourea (P7629; Sigma-Aldrich, St. Louis, MO, USA). Embryos were dechorionated by incubating them for 10 min in 1 ml of egg water after adding 100 μl of 10 mg/ml stock solution of Pronase (10165921001; Roche Applied Science, Laval, QC, Canada).

Generation of transgenic zebrafish lines and screening for transgene insertion by polymerase chain reaction and sequence analysis

For cloning the *actb2::KIT-D816V::2AeGFP* construct we used the previously available p5E-actb2 vector and pDestTol2pA2 destination vector (Tol2kit). p3E-T2A-EGFP was obtained from the laboratory of Dr Nathan Lawson (University of Massachusetts Medical School, Worcester, MA, USA). The KIT-D816V plasmid was kindly provided by Dr Gary Gilliland, (Abramson Family Cancer Research Institute, University of Pennsylvania, Philadelphia, PA, USA) and was used for making the middle-entry vector containing KIT-D816V without a stop codon, generated from a polymerase chain reaction (PCR) product amplified using primers CKIT-attB1f: 5′ggggacaagtttgtacaaaaaagcaggctcaatgagaggcgctcgcggc3′ and CKITattB2r: 5′ggggaccactttgtacaagaaagctgggtagacatcgtcg tgcacaag3′ and recombined with the pDONR221. The entry clone and whole vector recombination checking were performed as described before (Kwan *et al*, 2007). The *actb2::KIT-D816V::2AeGFP* construct was injected into zebrafish eggs at a concentration of 100 ng/μl, along with Tol2 transposase mRNA, also at 100 ng/μl (Fig 1A). Injected embryos were raised to adulthood (F0) and crossed to wild-type (AB strain) fish. Founder fish were identified by screening the F1

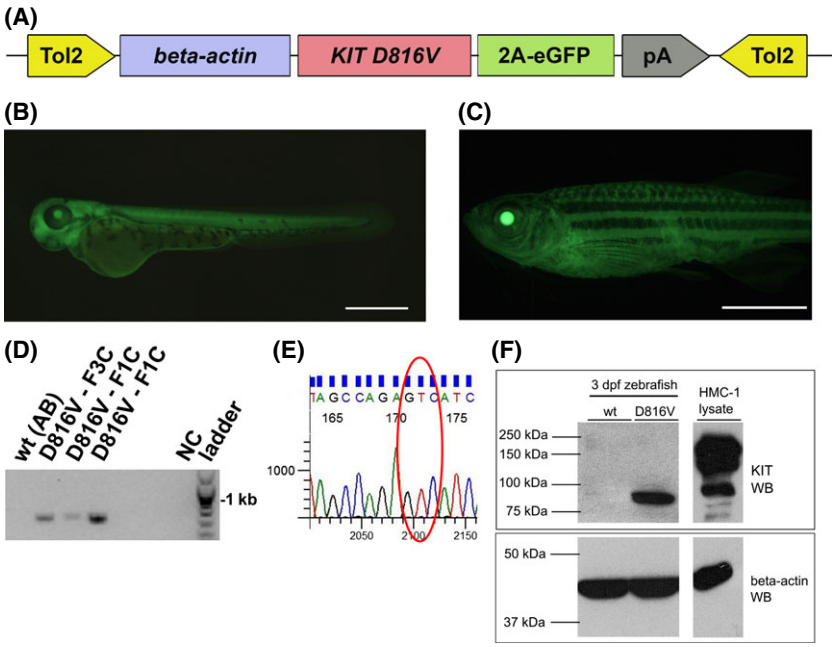

Fig 1. Transgenic zebrafish express human *KIT*-D816V ubiquitously under the control of the zebrafish *beta-actin* promoter. (A) Schematic representation of the *Tg(bactin::KIT-D816V::2AeGFP)* construct generated using the MultiSite Gateway® Technology. The human *KIT* gene with the D816V mutation was cloned between the ubiquitous zebrafish *beta-actin* promoter and green fluorescent protein (GFP) along with the viral co-translational cleavage peptide 2A. The final construct was flanked by Tol2 sites to facilitate transposase-mediated genomic integration. (B) Embryos were screened according to ubiquitous enhanced GFP (eGFP) expression. A 72 hpf *KIT*-D816V F4C transgenic embryo is shown (scale bar is 0·5 mm). (C) Ubiquitous eGFP expression was maintained into adulthood. A 12-month-old *KIT*-D816V F3C transgenic fish is shown (the scale bar is 0·5 cm). (D) PCR of genomic DNA extracted from *KIT*-D816V transgenic and wild type fish confirm the presence of the human *KIT* gene in the transgenic fish. (E) Sequencing traces of the PCR products from (D) displaying the g.2468A>T substitution corresponding to the p.D816V mutation, shown in red. (F) Anti-KIT Western blotting of 3 dpf wild-type and *KIT*-D816V transgenic larval lysates as well as of a positive control lysate from the HMC-1 human cell line known to express *KIT*-D816V (dpf = days post-fertilization). WB, Western blot.

offspring for ubiquitous green fluorescent protien (GFP) expression under a Leica MZ16F fluorescent microscope. Subsequent generations were maintained by crossing strongly positive transgenic fish. The ubiquitous GFP expression was observed into adulthood in about 70% of the fish.

The presence of the human *KIT*-D816V gene in transgenic zebrafish was confirmed by PCR and subsequent sequence analysis. A small part of the tail of an adult fish was clipped under anesthesia and sterile conditions. DNA was isolated from the fin clips using the REDExtract-N-Amp Tissue PCR Kit (XNATR-1KT; Sigma-Aldrich) according to the manufacturer's instructions. PCR was carried out using the following primers: *KIT2255F*: 5′aaagagatgtgactcccgcc3′, *KIT2942R*: 5′gacatcgtcgtgcacaagcag3′. Products of 683 bp were visualized on a 1% agarose gel and extracted from the gel for sequencing. The trace images were produced using the free Sequence Scanner software (Applied Biosystems, Foster City, CA, USA) of the 2468A>T substitution representing the D816V mutation.

Western blotting

Zebrafish embryos were deyolked as described previously (Westerfield, 2007) and lysed in the lysis buffer [10 mmol/l Tris-HCl, pH 7·4, and 1% sodium dodecyl sulfate (SDS)] containing Complete Protease Inhibitor Cocktail (11697498001; Roche Applied Science) and 1 mmol/l phenylmethanesulfonyl fluoride (PMSF) using 1-ml syringes with 22G needles. Proteins were resolved by SDS-polyacrylamide gel electrophoresis (SDS-PAGE) and transferred to a nitrocellulose membrane. Non-specific sites were blocked with 5% milk in Tris-buffered saline with Tween (TBST) before incubation with primary antibodies. We used anti-KIT antibodies (sc-365504; Santa Cruz Biotechnology, Santa Cruz, CA, USA) and anti-beta-actin antibodies (4967; Cell Signaling Technology, Danvers, MA, USA). Signals were detected SuperSignal West Pico substrate (34077; Fisher Scientific, Ottawa, ON, Canada) and exposure to X-ray film.

Whole mount in situ *hybridization assays*

Digoxigenin- and fluorescein-labelled RNA probes for zebrafish *cpa5*, *mpx*, *spi1b*, *csf1a*, *lcp1*, *gata1*, *hbbe3*, *gata2*, *cebpa*, were transcribed from linearized plasmids containing corresponding cDNAs according to manufacturer's protocol (11175025910; Roche Molecular Biochemicals, Indianapolis, IN, USA). Probes for *rrm2b*, *chtf18*, *rad23b*, *dnmt1*, *mt2* and *epcam* were transcribed from the PCR products containing a

T7 promoter (for sequences see Table SI). Whole mount *in situ* hybridization (WISH) assays were performed on embryos fixed in 4% paraformaldehyde at different time-points as described previously (Dobson *et al*, 2008). Images were taken on a Leica MZ16F microscope with a Leica DFC 490 camera (5× objective; Leica, Wetzlar, Germany). Micrographs are representative of at least two independent trials with 15–20 embryos per genotype.

Whole mount immunofluorescence assays for apoptosis and cell cycle

Fixed and permeabilized embryos were used to perform immunofluorescence (IF) for phosphorylated histone-H3 (pH3) as described in the literature with modifications (Shepard *et al*, 2004) or activated Caspase-3 (casp3) as per Jette *et al* (2008). The primary antibodies used were rabbit anti-p-Histone H3 (Ser10)-R IgG(sc-8656-R; Santa Cruz Biotechnology) and rabbit anti-Caspase-3, Active Form, (clone C92-605) IgG (559565; BD Pharmingen, Mississauga, ON, Canada). Secondary antibodies used were Alexa Fluor® 565 goat anti-rabbit/-mouse IgG (A-11011 and A11004; Life Technologies, Carlsbad, CA, USA). Z-stack projections for IF were captured on a Zeiss AxioObserver.Z1 microscope (5× and 10× objectives) with a Zeiss AxioCamHRm camera running ZEISS AXIOVISION, Release 4.8 software (Carl Zeiss Microimaging GmbH, Goettingen, Germany). Fluorescence micrographs were processed using MACBIOPHOTONICS IMAGEJ, Version 1.43 m (Sidi *et al*, 2008). Micrographs are representative of at least two independent trials with 15–20 embryos per genotype. Fluorescence images were quantified by applying the same threshold to all images to select only the most highly labelled cells and the labelled area was measured. Data are reported as mean values ± standard error of the mean (SEM). Statistical analysis was performed using two-tailed student's *t*-test.

Sectioning, histochemical stains and imaging

Adult fish were fixed in 10% neutral buffered formalin. Standard protocols were used for staining 5-μm sections for haematoxylin and eosin (H&E), Periodic Acid Schiff (PAS) and stains. Cytological and histopathological analysis of zebrafish sections was performed on-site at the IWK Health Centre. Tissue sections were visualized using an Olympus BX51 microscope (2×, 40×, and 100× objectives) with an Olympus DP25 colour camera (Olympus America Inc., Center Valley, PA, USA) and a Zeiss AxioObserver.Z1 microscope (5× and 10× objectives) with a Zeiss AxioCamHRm camera running ZEISS AXIOVISION, Release 4.8 software (Carl Zeiss Microimaging GmbH). Age of onset and prevalence of disease between different founder lines was analysed using a student's *t*-test and Fisher's exact test respectively with a P value $<0{\cdot}05$ considered significant.

Immunohistochemistry– tryptase staining protocol

Slides were deparaffinized and antigen retrieval was performed using 0·01 mol/l Na-Citrate Buffer, pH: 6·1 in a decloaking chamber (Biocare Medical, Concord, CA, USA). Endogenous peroxidase activity was quenched in 3% H_2O_2 in phosphate-buffered saline (PBS) for 10 min. Slides were then incubated with normal horse serum diluted 1:20 in PBS for 1 h at room temperature in a humid chamber. Tryptase primary antibody (M7052; Dako Canada, Burlington, ON, Canada) was diluted at 1:400 in PBS and applied to slides overnight in a humid chamber. Slides were washed three times in PBS between immunostaining steps and LSAB+ System-HRP Kit (K0689; Dako Canada) was applied according to manufacturer's directions. The reaction was visualized by using a liquid 3,3′-diaminobenzidine (DAB) + Substrate Chromogenic System (K3467; Dako Canada) and counterstained with Mayer's Haematoxylin. Slides were dehydrated through graded alcohols, xylene and mounted with Cytoseal TM60 for microscopic evaluation. Appropriate isotype negative and positive controls were performed to validate immunostain.

Adult zebrafish kidney dissections

Zebrafish adult kidneys were dissected according to Gerlach *et al* (2011). For microarray experiments, kidneys from three wild-type and from three diseased *KIT*-D816V adult zebrafish were dissected for RNA extraction. The age of wild-type adults was 18 months and that of *KIT*-D816V adult fish was approximately 24 months. The discrepancy between the ages of the two groups was due to availability constraints of aged wild-type strains at the time of the experiment. Kidney tissue was pooled for each group and used directly to extract RNA as below.

RNA isolation and microarray

RNA was extracted using a combination of the TRIzol (15596-026; Life Technologies) protocol and the RNeasy Mini Kit (74104; QIAGEN, Toronto, ON, Canada). Briefly, embryos or dissected kidneys were homogenized in TRIzol and centrifuged after treatment with chloroform to reveal the three-layered product. The supernatant containing RNA was precipitated in an equal volume of 70% ethanol and transferred into the spin columns of the RNeasy kit and purified according to manufacturer's instructions. Prior to use in labelling, RNA quality was assessed using the Experion bioanalyzer capillary electrophoresis system and total RNA standard sense chips (700-7153; Bio-Rad, Mississauga, ON, Canada) according to manufacturer's instructions. All RNA samples used in these experiments had RNA quality indices (RQI) of 8 or higher (out of 10) with corresponding low levels of degradation. Subsequently, 1 μg of each RNA sample

to be analysed was amplified using the Ambion Amino-Allyl-MessageAmp II aRNA amplification kit (AM1753; Life Technologies) according to the manufacturer's instructions. The quantity of amplified aRNA was assessed using the NanoDrop 2000 spectrophotometer (Nano-Drop; Thermo Scientific, Wilmington, DE, USA) and the quality and size distribution, were assessed by Experionbioanalyzer (Bio-Rad). The aRNA samples were then covalently labelled with AlexaFluor 555 or AlexaFluor 647 dyes as per kit instructions (A32756 and A32757; Life Technologies). Target aRNA yield and labelling efficiency were assessed by NanoDrop.

Two samples were used per hybridization mixture and were equalized for quantity (2 μg per sample) of labelled aRNA target added. Differences in labelling efficiencies of the two dyes were controlled through the use of dye swaps. Labelled target mixtures were fragmented for 30 min at 60°C using 25× fragmentation buffer – a component of the Agilent Gene Expression Hybridization kit (5188-5242; Agilent Technologies, Santa Clara, CA, USA). Following fragmentation, samples were made up to 60 μl with 2× GExHyb buffer (also a component of Agilent Gene Expression Hybridization kit). Samples were hybridized to Agilent 4x44k zebrafish V3 slides (design ID 026437, part number G2519F) using quad chambers on the TECAN HS4800 Pro instrument (Tecan, Durham, NC, USA). The hybridization protocol and program were as described for Agilent Two-Colour Microarray-Based Gene Expression Analysis with TECAN HS Pro hybridization. Briefly, samples were hybridized to slides for 17 h at 65°C with high agitation frequency. Slides were scanned at 5-μm resolution using a GenePix 4200AL scanner (Molecular Devices, Sunnyvale, CA, USA). Gridding was performed manually using SpotReader (Niles Scientific Inc., Sacramento, CA, USA) and the resulting GPR file was analysed using ACUITY 4 software (Molecular Devices). Data was imported and normalized using a whole slide Lowess normalization routine provided by Acuity. Analysis and quality control were assessed with Self-Organizing maps (SOM), Principal Component Analysis (PCA), *t*-test and volcano plotting of PCA scores *versus* log transformation of *t*-test scores. The top differentially expressed genes were extracted, compiled into lists and then compared between replicates. Gene Expression Omnibus microarray data are deposited under GSE54615 accession number and consists of embryonic (GSE54613) and adult data (GSE546134).

Quantitative real-time PCR

RNA was isolated as described above and treated with TurboDNAse using the TurboDNA-free kit (AM1907; Life Technologies). cDNA synthesis was performed using QuantiTect Reverse Transcription kit (205311; QIAGEN, Mississauga, ON, Canada) and quantitative real-time PCR (qRT-PCR) was performed using QuantiFast SYBR Green PCR kit (204154; QIAGEN) with theStratagene Mx3000PQPCR system and results were analysed using the MXPROQPCR Software (Agilent Technologies). Quantification was performed using the $2^{-\Delta\Delta C_t}$ method. The primers used are listed in Table SI. qPCR on genomic DNA from wild-type and transgenic adult fish was performed using 100 ng of DNA and primers for *EGFP* and *ryr3* (*ryanodine receptor 3*), an endogenous gene with a previously published qPCR assay (Dahlem *et al*, 2012). Primer efficiencies were estimated from a dilution series of genomic DNA from transgenic fish.

Gene Ontology pathway analysis

Database for Annotation, Visualization and Integrated Discovery (DAVID) was used to analyse enrichments of functional Gene Ontology terms. The gene sets were imported into DAVID web-based tool, processed using the standard pipeline and the results were downloaded.

Results

Ubiquitous expression of the human KIT *gene with the D816V mutation*

We used the Tol2 kit developed by the Chien Laboratory which utilizes the Gateway® system to generate transgenic expression constructs via recombination-based cloning (Kwan *et al*, 2007). The human *KIT*-D816V construct was cloned into the middle entry vector and the promoter-oncogene-fluorescent tag construct was assembled in a destination vector with flanking Tol2 sites. The *KIT*-D816V coding sequence was combined in-frame with the reporter enhanced GFP (eGFP) using the viral 2A linker, which allows for co-translational cleavage of the resulting polypeptide. Expression of the cassette was driven by the ubiquitous zebrafish *beta actin (actb2)* promoter (Fig 1).

After injection of the construct into zebrafish eggs and growing the positive embryos to adulthood, we identified three founders (designated A, B and C) whose homozygous offspring produced close to 100% GFP+ embryos. GFP expression was ubiquitous in all three transgenic lines. The B-line was discontinued due to poor survival of the founder and F1 generation fish. The A and C lines were maintained up to six generations and raised to adulthood. The C line was used for all embryo experiments, including WISH, immunofluorescence studies and microarray due to stronger expression of GFP in the embryos and availability of larger clutch sizes. Both A and C lines were used for adult studies, including kidney dissections and microarray, disease surveillance and histological analysis. There was only one adult fish from the B-line that was included in the total number. Expression of *KIT*-D816V was confirmed by PCR, Sanger sequencing and Western blot (Fig 1). qPCR on genomic DNA from adult transgenic fish for EGFP gene copy number relative to the copy number of an endogenous gene (*ryr3*) confirmed a single homozygous insertion of the transgene (data not shown).

Transgenic adults show signs of disease with evidence of increased numbers of mast cells in the kidney marrow

A total of 232 *Tg(actb2::KIT-D816V::2AeGFP)* transgenic zebrafish (heretofore referred to as the *KIT*-D816V line) were grown to adulthood and observed by regular daily surveillance for evidence of disease. At the time this manuscript was prepared, 144 (62%) fish had either died or been sacrificed at a median of 15 months (range 3–30 months). Twenty-eight of these fish (12% of total) were sacrificed while seemingly healthy for surveillance purposes. The remaining 116 (50% of total number of fish; 'prevalence') had either died spontaneously or been sacrificed because of various signs of disease (Fig 2). The median age of the latter group ('age of onset') was also 15 months (range 3–30 months). Between founder lines A and C, there was no statistically significant difference in median age of onset of disease, (16 [6–26] and 14 [3–30] months respectively, $P = 0{\cdot}11$) or disease prevalence (52·8% and 48·4% respectively, $P = 0{\cdot}57$).

The physical findings in sick fish included raised scales, distended abdomen, skin lesions and external bleeding ($n = 39$); thin and emaciated appearance with or without additional lesions ($n = 29$); and gross evidence of visceral masses ($n = 8$). Twenty (18%) of the sick fish were dissected for histological analysis. Of those 20, 12 fish (60%) had an abnormal histological appearance (Fig 2). Again, there was no statistically significant difference in the percentage of fish with abnormal histology between the founder lines (62·5% in the A-line vs. 58·3% in the C-line, $P = 1$).

The most common finding was kidney marrow expansion, with distortion of the normal tubular structures and an increased number of PAS-positive cells, suggesting a myeloid predominance (Fig 3. Compare E–G with A–C). Tryptase immunohistochemistry revealed increased numbers of positive cells in the kidney marrow compared to wild-type (Fig 3, compare H–D), supporting the idea that a proportion of the cells in the expanded myeloid compartment of the disorganized adult kidney marrow were mast cells. In several of the sick fish, findings were even more dramatic with complete effacement of normal kidney architecture and tremendous expansion of PAS+/tryptase+ cells that infiltrated into neighbouring organs, suggesting progression to a mast cell predominant myeloproliferative neoplasm (Fig 3I–L, Figure S1).

Microarray analysis of adult kidneys shows an increased expression of mast cell proteases in KIT-*D816V fish compared to wild-type*

To study mechanisms of adult haematopoietic disease phenotypes induced by *KIT*-D816V, we performed microarray experiments on pooled kidneys excised from normal wild-type and diseased *KIT*-D816V adults. The microarrays were performed on a single pooled sample from each genotype using two-colour dye-swap design. Genes showing the same

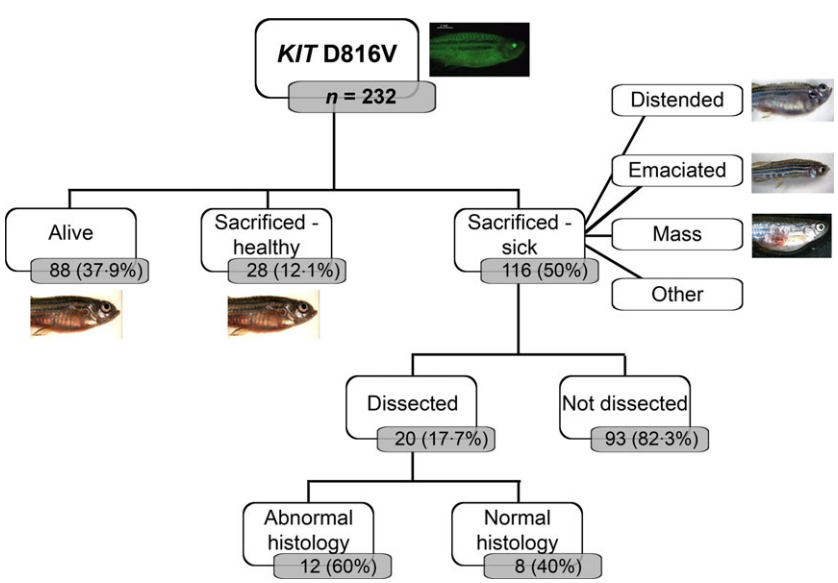

Fig 2. Flow chart of disease manifestations and pathology in adult *KIT*-D816V transgenic zebrafish demonstrates high prevalence of SM-like phenotype. Cross-sectional representation of macroscopic and microscopic findings in adult transgenic fish revealed a high prevalence of disease. Of the total number of transgenic fish ($n = 232$), half demonstrated obvious signs of disease; mostly in the form of distension, emaciation or visceral masses, as shown in representative images to the right of the boxes. 'Other' phenotypes included infections, skin lesions, bleeding from orifices or lesions, hypopigmentation and sickly appearance. A subset (17·7%) of the sick fish were sectioned for further analysis and 60% of these sectioned sick fish showed evidence of disease pathology, in the form of a myeloproliferative disease in the haematopoietic kidney marrow. The numbers and percentages are shown in grey boxes below each group. The percentage of each group refers to the ratio of that subset within the above group.

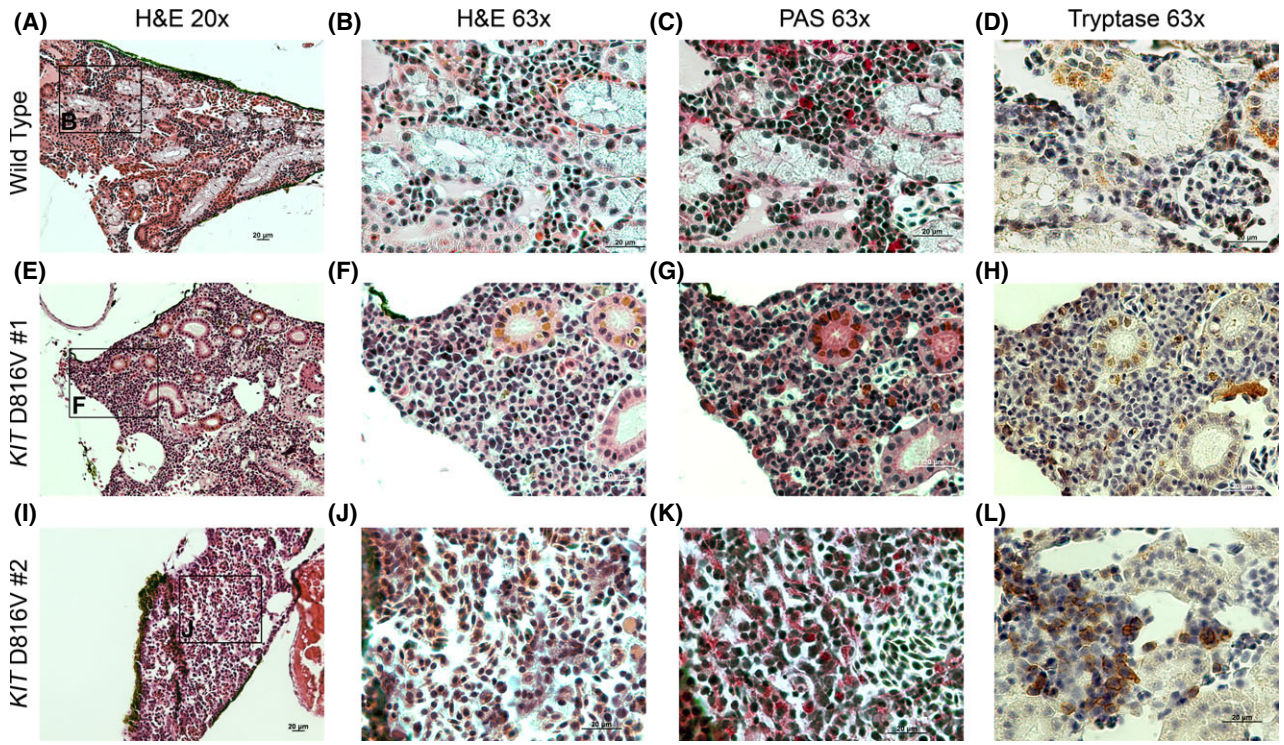

Fig 3. Adult *KIT*-D816V transgenic zebrafish exhibit a mast cell myeloproliferative phenotype in their kidney marrow. (A–D) In the wild type adult kidney, the organization of tubuli and glomeruli can be easily distinguished in H&E stained images (A, B); a few cells in the interstitium (C) are stained with Positive Acid Schiff (PAS+) and no tryptase-positive cells are present in this section (tubular cells take up non-specific stain) (D). (E–H) A 16-month-old female fish became sick and had a protruding lesion from its urogenital pore. Kidney marrow was expanded and disorganized, with increased numbers of PAS+ cells (E–G). Tryptase immunostaining was positive for a large proportion of cells in the kidney marrow (H). (I–L) A 6-month-old female fish grew a skin lesion on her back. The kidney was disorganized and the regular tubular structures were effaced (I, J). Increased numbers of PAS+ cells in the kidney marrow can be seen (K) as well as many cells positive for tryptase immunostaining (L).

direction (up or down) of differential expression in at least two microarray experiments were included in the final list of regulated genes. Strikingly, analysis of the differential genes between wild-type and *KIT*-D816V adult kidney datasets revealed 73 up-regulated genes, many of them encoding proteolytic enzymes typically expressed at high levels in mast cells and 71 down-regulated genes (Table SII). Gene Ontology analysis of the adult data set was also able to detect enrichment for 'proteolysis', 'metallopeptidase activity', 'serine endopeptidase activity' terms as well as a 'myofibril assembly' term which may be the result of a small muscle tissue contamination (Table I). These genomic findings suggest greater numbers of mast cells in adult kidneys of *KIT*-D816V fish, consistent with and complementing the pathology data presented in Fig 3.

Embryonic WISH studies reveal no prominent haematopoietic phenotype

By contrast to the adult phenotype, WISH analysis of *KIT*-D816V transgenic embryos at multiple developmental time points [from 12 h post-fertilization (hpf) to 7 d post-fertilization (dpf)] did not reveal a prominent change in haematopoietic markers. The mast cell specific marker, *cpa5*, was not increased at 28 hpf, the earliest time point when it is most robustly expressed (Dobson *et al*, 2008); or at later stages of development (48 and 72 hpf; 5 and 7 dpf). There was a slight increase in expression levels of the stem cell marker, *gata2* at 20 hpf (normal expression at 16, 24 and 28 hpf), and a decrease in expression was observed for the early pan-myeloid marker *spi1b*, most prominently at 24 hpf. No changes in expression were observed for additional myeloid (*mpx*, *lcp1*, *csf1ra*, *cebpa*) or erythroid markers (*hbbe3*, *gata1*) (Figure S2).

Hyperactive KIT perturbs cell-cycle progression and increases apoptosis levels in transgenic embryos

Whole mount apoptosis and cell cycle assays were performed on transgenic embryos as well as on wild type AB control embryos. Apoptosis levels were examined using active Caspase 3 staining in 28 hpf embryos. Imaging of active Caspase 3 (Fig 4A) followed by intensity threshold-based statistical analysis of labelled area fractions revealed a small but significant increase in apoptosis levels in *KIT*-D816V compared to wild-type embryos (Fig 4B). To investigate the effects of

Table I. Enriched Gene Ontology terms in the biological process and molecular function categories.

Term – biological process	Count	*P*-value	Genes
GO:0006508 – proteolysis	20	$1{\cdot}0 \times 10^{-6}$	*zgc:92511*, *zgc:92590*, *cpa4*, *zgc:112368*, *zgc:112160*, *ctrb1*, *c6ast3*, *ttnb*, *c6ast4*, *zgc:66382*, *zgc:112302*, *zgc:136461*, *ufm1*, *zgc:92041*, *ela2l*, *try*, *ela2*, *cpb1*, *ela3l*, *ctrl*
GO:0030239 – myofibril assembly	4	$6{\cdot}9 \times 10^{-11}$	*myl7*, *cmlc1*, *ttnb*, *tpm4*

Term – molecular function	Count	*P*-value	Genes
GO:0004252 – serine-type endopeptidase activity	14	$7{\cdot}7 \times 10^{-3}$	*zgc:92590*, *zgc:92511*, *zgc:112368*, *zgc:112160*, *ctrb1*, *zgc:66382*, *zgc:112302*, *zgc:136461*, *zgc:92041*, *ela2l*, *ela2*, *try*, *ela3l*, *ctrl*
GO:0015082 – di-, tri-valent inorganic cationtransmembrane transporter activity	3	$2{\cdot}8 \times 10^{-2}$	*atp2a1l*, *slc39a13*, *atp2a2a*
GO:0005509 – calcium ion binding	9	$2{\cdot}9 \times 10^{-2}$	*pvalb4*, *myl7*, *pvalb3*, *cmlc1*, *actn3a*, *mylz3*, *mylz2*, *tnnc*, *stnnc*
GO:0005529 – sugar binding	4	$3{\cdot}5 \times 10^{-2}$	*zgc:153499*, *si:ch211-226h8.4*, *si:ch211-154a22.8*, *si:dkeyp-46h3.2*, *si:ch211-226h8.11*, *zgc:172053*
GO:0008237 – metallopeptidase activity	4	$7{\cdot}4 \times 10^{-2}$	*cpa4*, *c6ast3*, *c6ast4*, *cpb1*
GO:0005388 – calcium-transporting ATPase activity	2	$7{\cdot}7 \times 10^{-2}$	*atp2a1l*, *atp2a2a*

KIT-D816V on cell cycle progression leading to mitosis (G2 to M phase transition), we completed phospho-S10 histone H3 (pH3) labelling at 28 and 48 hpf (Shepard *et al*, 2004). Using similar imaging and analysis techniques, a consistent and significant decrease in pH3 labelling was observed in transgenic compared to wild type embryos at both 28 and 48 hpf (Fig 4C, D), suggesting a cell-cycle progression defect in the transgenic embryos in the context of a constitutively active KIT background.

Pattern of differentially expressed genes in KIT-*D816V embryos reflects an altered cell cycle phenotype*

To gain insight into potential molecular mechanisms of cell-cycle effects and to identify *KIT*-D816V-regulated genes, we conducted microarray expression profiling of 28 hpf embryos of wild-type and *KIT*-D816V genotypes. This time point was chosen to correspond with the timing of mast cell development, because 28 hpf is the earliest time point when *cpa5*-positive mast cells are easily and robustly detectable (Dobson *et al*, 2008). Microarray experiments were performed on 28 hpf embryos four times using two-colour channel swap microarray design, with evaluation as above for gene expression differences in adult transgenic fish. There were 23 up-regulated and 47 down-regulated genes (Table SIII). The overlap of the embryonic dataset with the set of adult regulated genes was only seven genes (*epcam*, *rrs1*, *dnmt1*, *ube2c*, *pdf*, *zgc:195170*, *si:dkey-23c22.6*).We also studied pathway and Gene Ontology term enrichment for this dataset, but did not identify significant groups of genes, probably due to the small number of regulated genes. We verified 11 genes (*cyp1a*, *rrs1*, *srsf5a*, *ccl-c25v*, *rrm2b*, *ndrg4*, *chtf18*, *rad23b*, *dnmt1*, *mt2*, *epcam*) with identifiable functions by qPCR, and seven of these genes (Fig 5A) could be consistently confirmed. We further performed WISH for the up-regulated genes: *rrm2b*, *chtf18* and *rad23b* as well as for the down-regulated genes: *dnmt1*, *mt2* and *epcam*. Consistent increases of WISH signal in *KIT*-D816V embryos were observed for *rrm2b*, *chtf18* and *rad23b* (Fig 5B). Interestingly, Rrm2b is required for DNA repair in quiescent cells and mitochondrial DNA maintenance (Pontarin *et al*, 2012). Two other up-regulated genes, *rad23b* and *chtf18*, are also involved in DNA repair, where Rad23b regulates nucleotide excision repair (Ng *et al*, 2003), while Chtf18 is required for DNA polymerase epsilon loading onto DNA (Ogi *et al*, 2010). Thus, changes in expression of these genes may be related to the cell cycle phenotypes in *KIT*-D816V embryos we observed (Fig 4). WISH with probes for the down-regulated genes also showed expression differences for *mt2*, *dnmt,* and *epcam* genes (Fig 5B). Metallothionein 2 (Mt2) is involved in protection against heavy metals, oxidative stress and promoting cell survival (Swindell, 2011). It is expressed in wild-type embryos at 28 hpf in cells covering the yolk, as well as some unknown cells of probable haematopoietic origin, as this is one of the known expression domains in the mouse as reviewed in (Swindell, 2011). Expression of *mt2* was strongly decreased in *KIT*-D816V transgenic zebrafish embryos (Fig 5B).

Functional follow-up of dnmt1 *and* epcam *down-regulation in 28 hpf* KIT-*D816V transgenic embryos*

Dnmt1 (DNA methyltransferase I) is the principal enzyme responsible for maintaining CpG island methylation and along with other DNA methyltransferases, has been implicated in haematopoietic and leukaemic stem cell renewal (Trowbridge *et al*, 2009, 2012). Interestingly, *dnmt1* was consistently down-regulated in both embryonic and adult microarray datasets and its regulation was confirmed by qPCR and by WISH in embryos (Fig 5). By contrast, comparable levels of DNA methylation were observed in wild-type and *KIT-D816V* embryos analysed both by restriction digest and antibody-based slot-blot techniques (data not shown). Thus, the

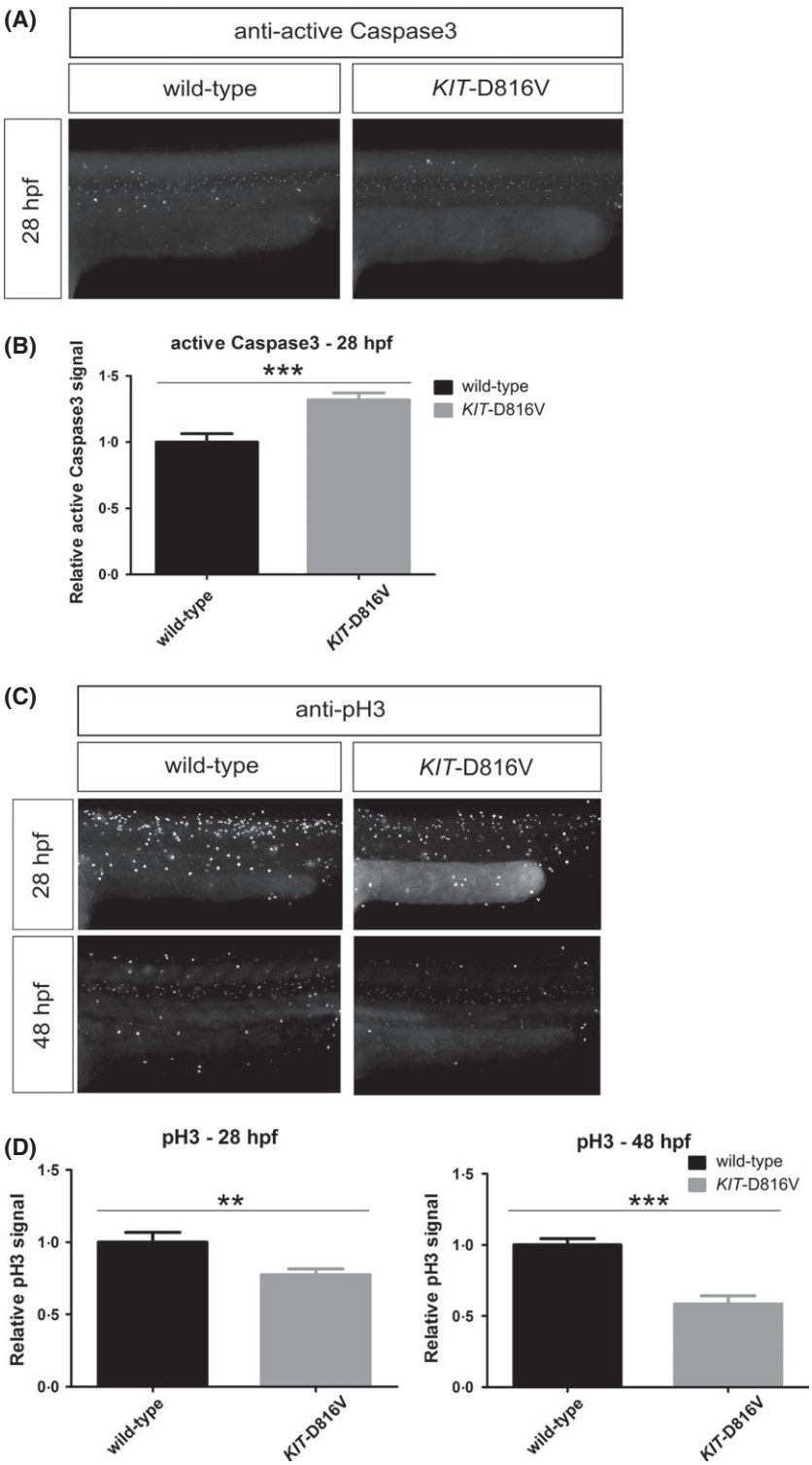

Fig 4. Cell cycle and apoptosis assays suggest an increase in apoptosis and a putative block in G2/M transition in *KIT*-D816V transgenic embryos. (A) Active Caspase 3 labelling of wild-type and *KIT-D816V* transgenic embryos at 28 hpf. Staining was completed on a total of 50 embryos for each genotype in three independent experiments and representative images are shown. Embryos are displayed in side profile, anterior to the left. (B) Statistical analysis of the labelled area fractions relative to wild-type shows an increase in the active Caspase 3 labelling in *KIT*-D816V transgenic embryos (***P-value <0·001). (C) G2/M cells were labelled by anti-phospho-histone H3 (pH3) antibody staining in wild-type and *KIT*-D816V transgenic embryos at 28 and 48 hpf. Representative images show magnified views of the tail region used for quantification. Embryos are displayed in side profile, anterior to the left. (D) Quantification of anti-phospho-histone H3 staining in wild-type and *KIT*-D816V embryos at 28 and 48 hpf shows a decrease in mean relative pH3-labelled area fractions at both stages. The analysis was performed at 28 hpf on 23 wild-type and 26 *KIT*-D816V embryos (**t-test P-value <0·01) and at 48 hpf on 35 wild-type and 49 *KIT*-D816V embryos (***t-test P-value <0·001), in two independent experiments at both stages. (hpf = hours post-fertilization).

decrease in *dnmt1* expression in *KIT*-D816V embryos did not result in significant changes in global methylation. However, we cannot exclude other effects of *dnmt1* decrease on gene expression.

Down-regulation of the *epcam* gene in *KIT*-D816V fish was observed in both embryonic and adult microarray datasets, suggesting that this gene is highly responsive to activity of *KIT*-D816V in zebrafish. We also were able to confirm its lower expression level by both qPCR and WISH in embryos (Fig 5). Expression of *epcam* was reduced in most of its expression domains such as the epidermis, gastrointestinal tract, lateral line system and olfactory region

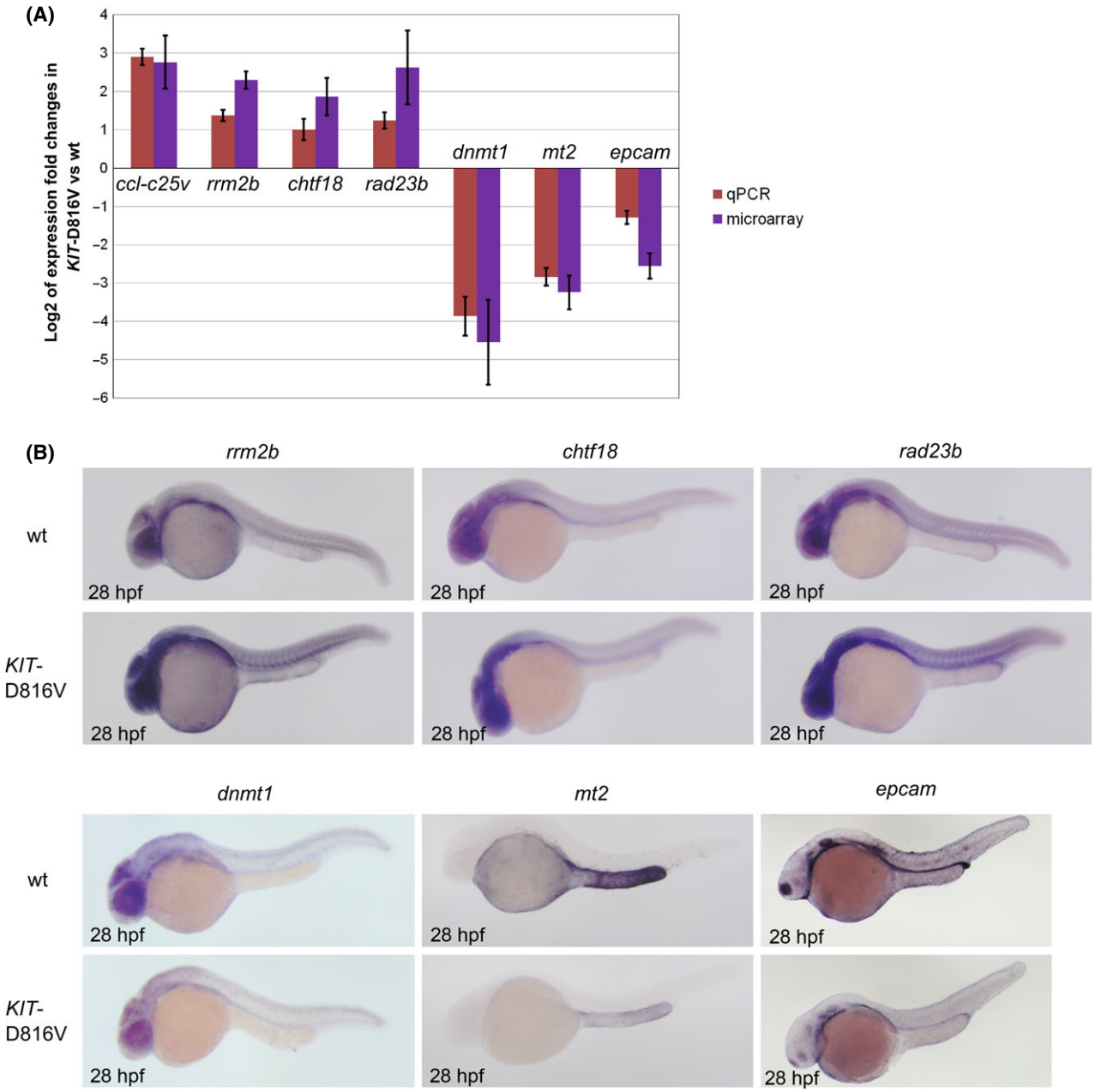

Figure 5. Confirmation of selected differentially expressed genes between 28 hpf wild-type and *KIT*-D816V embryos identified by microarray-based gene expression profiling. (A) Changes of expression (log2 fold changes) of *ccl-c25v*, *rrm2b*, *chtf18*, *rad23b*, *dnmt1*, *mt2* and *epcam* genes identified by microarray and quantitative PCR (qPCR). The values for microarray experiments are from 2 to 4 hybridizations and for qPCR are from three independent experiments. Mean and standard deviations are shown in the graph. (B) Whole mount *in situ* hybridisation (WISH) assays for *rrm2b*, *chtf18*, *rad23b* (up-regulated), *dnmt1*, *mt2* and *epcam* (down-regulated) genes in wild type (wt) and *KIT*-D816V zebrafish embryos were performed on 30 embryos in two independent experiments and the representative images are shown.

(Fig 5B). Although *epcam* is not known to be directly involved in mast cell biology and function, it has several roles in regulating cell adhesion, functions as a transcription factor and promotes cell proliferation and tumour growth (Schnell *et al*, 2013). In zebrafish, knock-down of *epcam* results in defects in the lateral line primordium migration and reduced deposition of neuromast groups of sensory cells (Villablanca *et al*, 2006). We used enumeration of neuromasts to assess if expression of *KIT*-D816V has a biological effect in this context. There was indeed a significant reduction in the number of visually discernible neuromasts in *KIT*-D816V embryos and their sizes were typically smaller (Fig 6). While this finding requires additional evaluation in the context of *KIT*-D816V function, it provides an easy and rapid visual read-out of *KIT*-D816V effects in our transgenic model.

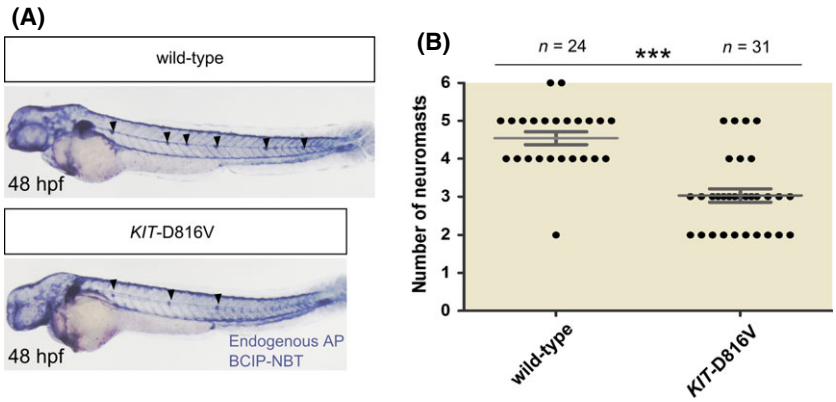

Fig 6. Neuromast quantification in 48 hpf wild-type and *KIT*-D816V embryos. (A) Representative examples of 48 hpf wild-type and *KIT*-D816V embryos stained with nitro-blue tetrazolium and 5-bromo-4-chloro-3′-indolyphosphate (NBT-BCIP) to detect endogenous alkaline phosphatase (AP) are shown. Neuromasts are marked with the black triangles. (B) Neuromasts were manually counted on a single side in 24 wild-type and 31 *KIT*-D816V embryos in two independent experiments, and the data from both experiments was combined demonstrating a significant decrease in the transgenic embryos (***indicates statistical significance <0·001, which in this case was P = 4·98*10e-6 by non-parametric Mann–Whitney test). Mean and standard errors are shown in the graph.

Discussion

Here we describe the first zebrafish model of human SM, employing the human *KIT*-D816V mutant gene under a ubiquitous zebrafish promoter. Use of the human gene construct predicts greater fidelity and reliability in the translation of results observed for collaborating molecular pathways and responses to therapy. Confirmation of germline expression and penetrance of disease phenotype in our adult transgenic fish dispels previously raised concerns regarding embryonic lethality of animal models with germline expression of human *KIT*-D816V and more subtle manifestations of disease due to limited conservation of cross-species intracellular signalling (Gerbaulet *et al*, 2011). The incidence of disease in our transgenic zebrafish expressing human *KIT*-D816V is significantly greater than in the transgenic mice overexpressing the same human mutant gene observed in an earlier study (50% vs. 30%) albeit with similar disease latency (Zappulla *et al*, 2005). Of the diseased fish that were dissected, a significant proportion (60%) showed abnormal histology in the form of myeloproliferation and mast cell expansion. Because it was technically not feasible to dissect all fish with signs of disease (n = 116), we can only postulate that this percentage reflects the actual disease prevalence in our line. The absence of overt disease by histology in 40% of fish may be due to a number of reasons. In the case of two of these eight fish, the tissues were too disintegrated to effectively analyse the number of myeloid cells in the kidney marrow, as the presentation of these fish was 'sudden death'. We have classified these fish under 'normal histology' due to lack of an overt disease that could be appreciated in the sections. In the remainder of fish, we can speculate that the difference in phenotype is in keeping with the extensive clinical variability of human SM in adults, ranging from indolent to a fulminant myeloproliferative disease.

Despite the phenotypic variability, these transgenic fish represent the first animal model with clinical features in keeping with aggressive SM or mast cell leukaemia (MCL), with accumulation of mast cells and a myeloproliferative neoplasm (MPN)-like phenotype specifically in the kidney marrow, features not seen in transgenic mice overexpressing either human *KIT*-D816V or the more potent murine *Kit*-D814V (Gerbaulet *et al*, 2011). Mice expressing *Kit*-D814V also exhibited some unusual disease characteristics not entirely in keeping with the human disease, such as an embryonic lethal hyperproliferative erythroid dysregulation in non-inducible transgenic animals, concurrent prominent B-precursor acute leukaemia, and intestinal inflammation (Gerbaulet *et al*, 2011). By contrast, expression of human *KIT*-D816V early in development using the β-actin promoter did not result in these manifestations in our zebrafish model. In fact, as was observed in transgenic mouse embryos expressing human *KIT*-D816V (Zappulla *et al*, 2005), our transgenic zebrafish embryos did not demonstrate any signs of mast cell pathology, as evidenced by no decrease in overall survival and normal embryonic haematopoiesis. The latency of a mastocytosis phenotype in transgenic embryos may reflect the potency of the oncogenic signal or may be related to the choice of promoter. Currently, no exclusive mast cell-expressing promoters are available in the zebrafish. We have been developing a *cpa5*-based knock-in of a fluorescent protein gene or an exogenous transcription factor gene such as Gal4 using clustered regularly interspaced short palindromic repeats (CRISPRs) (S.V. Prykhozhij and J.N. Berman, unpublished data). The β-actin promoter was chosen on account of its track record in generating haematopoietic malignancies and in particular, its efficacy in promoting pre-B ALL in a model of *ETV6-RUNX1* -driven leukaemia, when the lymphoid-specific *rag2* promoter was unsuccessful (Sabaawy *et al*, 2006). This study suggested that the use of ubiquitous promoters active earlier in zebrafish blood development may prove more robust at driving leukaemic transformation. Despite an early disease manifestation in this study, incidence

was very low at 3% of fish, which is in contrast to the high penetrance but late onset of *KIT*-D816V expressing fish seen in our study. These data indicate the importance of careful interpretation of manifestations when using a ubiquitous promoter and raises the question of whether a mast cell-specific promoter may result in an earlier, more robust disease phenotype.

A unique opportunity afforded by the zebrafish model is the ability to compare embryonic and adult phenotypes of a transgenic system to unravel the putative transforming events in the course of a disease. The high genomic conservation and local synteny between the human and zebrafish genomes make genome-scale analysis by microarray a powerful method for translational research and medical discovery. However, the choice of promoter in our transgenic model may have similarly had an impact on the relatively few genes differentially expressed in zebrafish embryos overexpressing *KIT*-D816V. The ubiquitous expression may have led to incompatible signalling adapters and downstream molecules, as well as potential masking of significant expression changes in specific tissues. While a specific mast cell or haematopoietic phenotype was not observed in *KIT-D816V* embryos either by WISH or microarray, down-regulation of *epcam* and decreased numbers of neuromasts provides a consistent surrogate assay that could be employed in an embryonic chemical screen to identify compounds that restore normal *epcam*/neuromast expression. Such a compound, in turn, may have the potential to impact the biological effects of *KIT* overexpression found in human mast cell diseases harbouring the D816V mutation. This is particularly relevant, given the strong aggressive mastocytosis phenotype observed in adult *KIT*-D816V transgenic fish, which also exhibit down-regulation of *epcam*. The most upregulated genes in adult affected kidneys were endopeptidases, mirroring microarray results from the bone marrows of human mastocytosis patients (D'ambrosio *et al*, 2003), although we did not similarly observe increased expression levels of oncogenes, cell cycle genes or haematopoietic transcription factors, such as *gata2*.

KIT-D816V transgenic embryos also demonstrated evidence of a cell-cycle defect, which ultimately would need to be overcome later in development to result in the proliferative mast cell disorder observed in adult fish. Interestingly, we have described another transgenic zebrafish line overexpressing the human *NUP98-HOXA9* transgene found in high risk acute myeloid leukaemia that similarly develops an MPN phenotype in the adult kidney marrow (Forrester *et al*, 2011). In contrast to the *KIT*-D816V line, *NUP98-HOXA9* embryos demonstrated no increase in BrdU or pH3 labelling under steady-state conditions, but in fact have significantly elevated *dnmt1* expression (Deveau *et al*, 2012). While the functional significance of decreased *dnmt1* expression remains to be elucidated in the *KIT*-D816V model, these contrasting findings suggest different mechanisms and roles of epigenetic regulation in these two transgenic zebrafish models resulting in an adult MPN phenotype.

Given its similarity to chronic myeloid leukaemia regarding a constitutively active tyrosine kinase as an underlying molecular pathology, SM with a *KIT*-D816V mutation has been the subject of many clinical trials with known and novel tyrosine kinase inhibitors, as reviewed in Ustun *et al* (2011) and Pardanani (2012), however it remains a disease without a definitive cure. With the overall results of these targeted therapies being far from satisfactory, there is a clear need for additional models to better elucidate disease pathogenesis and enable high-throughput *in vivo* drug testing. The time and expense required for many of the current mouse models of myeloproliferative diseases and leukaemia have hampered the application of the mouse model system. These challenges have also encouraged the emergence of the zebrafish, largely owing to the distinct advantages afforded by the large numbers of rapidly-developing externally-fertilized embryos that can be easily manipulated and subjected to large-scale chemical modifier screens. While there are limitations with regards to the expression data described above that can be improved upon in future transgenic models by incorporating mast cell-specific promoters and other genetic enhancers, the transgenic zebrafish model presented here recapitulates features of aggressive human SM in the adult kidney marrow and provides embryonic surrogate markers that could be utilized in drug testing. Importantly, it represents the first zebrafish model of a human mast cell disease and hearkens at the potential of this versatile vertebrate system to provide new insights on the pathogenesis and putative novel therapies for SM and other MPNs.

Acknowledgements

The authors would like to thank Dr Gary Gilliland for providing the *KIT*-D816V construct, Pat Colp for assistance with the tryptase immunostaining, Andrew Coombs for husbandry and care of zebrafish, preparation of reagents and help with experiments, Dr Kirsten Sadler Edepli as well as her laboratory members, Yelena Chernyavskaya and Raksha Mudbhary, for methylation analyses.

Funding

This research was funded by a Canadian Institutes of Health Research operating grant 287512.

Competing interest statement

The authors declare no competing interests.

Author contributions

T.B.B. and S.V.P. designed and performed the experiments, analysed data, prepared the figures and wrote the manuscript. E.M.T. built the construct and generated the transgenic line. S.I.D. provided guidance and helped with various experiments. E.M. and R.L. provided expertise in the analysis of histology

samples. I.C, D.L. and S.L. performed and analysed the microarray experiments. J.N.B. conceived of the study design, developed the concepts, wrote and edited the manuscript.

Supporting Information

Additional Supporting Information may be found in the online version of this article:

Figure S1. Adult KIT-D816V transgenic zebrafish developed a kidney marrow mass with an abundance of myeloid cells invading neighboring structures.

Figure S2. WISH analysis of the KIT-D816V line at multiple developmental time points did not reveal a prominent change in hematopoietic markers.

Table SI. Primers used in the study and their applications.

Table SII. Regulated genes in transgenic *actb2:hCKIT-2A-EGFP* relative to wild-type control zebrafish embryos at 28 hpf microarray datasets.

Table SIII. Regulated genes in transgenic *actb2:hCKIT-2A-EGFP* relative to wild-type control adult kidneys microarray results.

References

Berman, J., Hsu, K. & Look, A.T. (2003) Zebrafish as a model organism for blood diseases. *British Journal of Haematology*, **123**, 568–576.

Burns, C.G., Milan, D.J., Grande, E.J., Rottbauer, W., MacRae, C.A. & Fishman, M.C. (2005) High-throughput assay for small molecules that modulate zebrafish embryonic heart rate. *Nature Chemical Biology*, **1**, 263–264.

Chen, E.Y. & Langenau, D.M. (2011) Zebrafish models of rhabdomyosarcoma. *Methods in Cell Biology*, **105**, 383–402.

Da'as, S., Teh, E.M., Dobson, J.T., Nasrallah, G.K., McBride, E.R., Wang, H., Neuberg, D.S., Marshall, J.S., Lin, T.-J. & Berman, J.N. (2011) Zebrafish mast cells possess an FcεRI-like receptor and participate in innate and adaptive immune responses. *Developmental and Comparative Immunology*, **35**, 125–134.

Da'as, S.I., Coombs, A.J., Balci, T.B., Grondin, C.A, Ferrando, A.A & Berman, J.N. (2012) The zebrafish reveals dependence of the mast cell lineage on Notch signaling in vivo. *Blood*, **119**, 3585–3594.

Dahlem, T.J., Hoshijima, K., Jurynec, M.J., Gunther, D., Starker, C.G., Locke, A.S., Weis, A.M., Voytas, D.F. & Grunwald, D.J. (2012) Simple methods for generating and detecting locus-specific mutations induced with TALENs in the zebrafish genome. *PLoS Genetics*, **8**, e1002861. Available at: http://www.pubmedcentral.nih.gov/articlerender.fcgi?artid=3420959&tool=pmcentrez&rendertype=abstract [Accessed April 30, 2014].

D'ambrosio, C., Akin, C., Wu, Y., Magnusson, M.K. & Metcalfe, D.D. (2003) Gene expression analysis in mastocytosis reveals a highly consistent profile with candidate molecular markers. *The Journal of Allergy and Clinical Immunology*, **112**, 1162–1170.

Deveau, A., Forrester, A.M., Grabher, C., Coombs, A.J., Chute, I., Leger, D., Lewis, S., Look, A.T. & Berman, J.N. (2012) Epigenetic therapy inhibits NUP98-HOXA9-mediated myeloid disease – decitabine and valproic acid work synergistically to rescue normal hematopoiesis in transgenic zebrafish. *Blood (ASH Annual Meeting Abstracts)*, **120**, 2391.

Dobson, J.T., Seibert, J., Teh, E.M., Da'as, S., Fraser, R.B., Paw, B.H., Lin, T.-J. & Berman, J.N. (2008) Carboxypeptidase A5 identifies a novel mast cell lineage in the zebrafish providing new insight into mast cell fate determination. *Blood*, **112**, 2969–2972.

Forrester, A.M., Grabher, C., McBride, E.R., Boyd, E.R., Vigerstad, M.H., Edgar, A., Kai, F.-B., Da'as, S.I., Payne, E., Look, A.T. & Berman, J.N. (2011) NUP98-HOXA9-transgenic zebrafish develop a myeloproliferative neoplasm and provide new insight into mechanisms of myeloid leukaemogenesis. *British Journal of Haematology*, **155**, 167–181.

Gerbaulet, A., Wickenhauser, C., Scholten, J., Peschke, K., Drube, S., Horny, H.-P., Kamradt, T., Naumann, R., Müller, W., Krieg, T., Waskow, C., Hartmann, K. & Roers, A. (2011) Mast cell hyperplasia, B-cell malignancy, and intestinal inflammation in mice with conditional expression of a constitutively active kit. *Blood*, **117**, 2012–2021.

Gerlach, G.F., Schrader, L.N. & Wingert, R.A. (2011) Dissection of the adult zebrafish kidney. *Journal of Visualized Experiments: JoVE*, **54**, 1–5.

Jette, C.A., Flanagan, A.M., Ryan, J., Pyati, U.J., Carbonneau, S., Stewart, R.A., Langenau, D.M., Look, A.T. & Letai, A. (2008) BIM and other BCL-2 family proteins exhibit cross-species conservation of function between zebrafish and mammals. *Cell Death and Differentiation*, **15**, 1063–1072.

Jing, L. & Zon, L.I. (2011) Zebrafish as a model for normal and malignant hematopoiesis. *Disease Models & Mechanisms*, **4**, 433–438.

Kwan, K.M., Fujimoto, E., Grabher, C., Mangum, B.D., Hardy, M.E., Campbell, D.S., Parant, J.M., Yost, H.J., Kanki, J.P. & Chien, C.-B. (2007) The Tol2kit: a multisite gateway-based construction kit for Tol2 transposon transgenesis constructs. *Developmental Dynamics: An Official Publication of the American Association of Anatomists*, **236**, 3088–3099.

Langenau, D.M., Traver, D., Ferrando, A.A., Kutok, J.L., Aster, J.C., Kanki, J.P., Lin, S., Prochownik, E., Trede, N.S., Zon, L.I. & Look, A.T. (2003) Myc-induced T cell leukemia in transgenic zebrafish. *Science*, **299**, 887–890.

Longley, J.B., Tyrell, L., Lu, S.-Z., Ma, Y.-S., Langley, K., Ding, T., Duffy, T., Jacobs, P., Tang, L.H. & Modlin, I. (1996) Somatic c-KIT activating mutation in urticaria pigmentosa and aggressive mastocytosis: establishment of clonality ina human mast cell neoplasm. *Nature Genetics*, **12**, 312–314.

Martin, P. & Feng, Y. (2009) Inflammation: wound healing in zebrafish. *Nature*, **459**, 921–923.

Metcalfe, D.D. (2008) ASH 50th anniversary review Mast cells and mastocytosis. *Blood*, **112**, 946–956.

Metcalfe, D.D. & Akin, C. (2001) Mastocytosis: molecular mechanisms and clinical disease heterogeneity. *Leukemia Research*, **25**, 577–582.

Nagata, H., Worobec, A.S., Oh, C.K., Chowdhury, B.A., Tannenbaum, S., Suzuki, Y. & Metcalfe, D.D. (1995) Identification of a point mutation in the catalytic domain of the protooncogene c-kit in peripheral blood mononuclear cells of patients who have mastocytosis with an associated hematologic disorder. *Proceedings of the National Academy of Sciences of the United States of America*, **92**, 10560–10564.

Ng, J.M.Y., Vermeulen, W., van der Horst, G.T.J., Bergink, S., Sugasawa, K., Vrieling, H. & Hoeijmakers, J.H.J. (2003) A novel regulation mechanism of DNA repair by damage-induced and RAD23-dependent stabilization of xeroderma pigmentosum group C protein. *Genes & Development*, **17**, 1630–1645.

North, T.E., Goessling, W., Walkley, C.R., Lengerke, C., Kopani, K.R., Lord, A.M., Weber, G.J., Bowman, T.V., Jang, I.-H., Grosser, T., Fitzgerald, G.A., Daley, G.Q., Orkin, S.H. & Zon, L.I. (2007) Prostaglandin E2 regulates vertebrate haematopoietic stem cell homeostasis. *Nature*, **447**, 1007–1011.

Ogi, T., Limsirichaikul, S., Overmeer, R.M., Volker, M., Takenaka, K., Cloney, R., Nakazawa, Y., Niimi, A., Miki, Y., Jaspers, N.G., Mullenders, L.H.F., Yamashita, S., Fousteri, M.I. & Lehmann, A.R. (2010) Three DNA polymerases, recruited by different mechanisms, carry out NER repair synthesis in human cells. *Molecular Cell*, **37**, 714–727.

Pardanani, A. (2012) Systemic mastocytosis in adults: 2012 update on diagnosis, risk stratification, and management. *American Journal of Hematology*, **87**, 401–411.

Patnaik, M.M., Rindos, M., Kouides, P.A, Tefferi, A. & Pardanani, A. (2007) Systemic mastocytosis: a concise clinical and laboratory review. *Archives of Pathology & Laboratory Medicine*, **131**, 784–791.

Patton, E.E., Widlund, H.R., Kutok, J.L., Kopani, K.R., Amatruda, J.F., Murphey, R.D., Berghmans,

S., Mayhall, E.A., Traver, D., Fletcher, C.D.M., Aster, J.C., Granter, S.R., Look, A.T., Lee, C., Fisher, D.E. & Zon, L.I. (2005) BRAF mutations are sufficient to promote nevi formation and cooperate with p53 in the genesis of melanoma. *Current Biology: CB*, **15**, 249–254.

Peterson, R.T., Link, B.A., Dowling, J.E. & Schreiber, S.L. (2000) Small molecule developmental screens reveal the logic and timing of vertebrate development. *Proceedings of the National Academy of Sciences of the United States of America*, **97**, 12965–12969.

Pontarin, G., Ferraro, P., Bee, L., Reichard, P. & Bianchi, V. (2012) Mammalian ribonucleotide reductase subunit p53R2 is required for mitochondrial DNA replication and DNA repair in quiescent cells. *Proceedings of the National Academy of Sciences of the United States of America*, **109**, 13302–13307.

Renshaw, S.A. & Trede, N.S. (2012) A model 450 million years in the making: zebrafish and vertebrate immunity. *Disease Models & Mechanisms*, **5**, 38–47.

Ribatti, D., Crivellato, E., Roccaro, A.M., Ria, R. & Vacca, A. (2004) Mast cell contribution to angiogenesis related to tumour progression. *Clinical and Experimental Allergy: Journal of the British Society for Allergy and Clinical Immunology*, **34**, 1660–1664.

Ribatti, D., Crivellato, E. & Molica, S. (2009) Mast cells and angiogenesis in haematological malignancies. *Leukemia Research*, **33**, 876–879.

Robyn, J. & Metcalfe, D.D. (2006) Systemic mastocytosis. *Advances in Immunology*, **89**, 169–243.

Sabaawy, H.E., Azuma, M., Embree, L.J., Tsai, H. J., Starost, M.F. & Hickstein, D.D. (2006) TEL-AML1 transgenic zebrafish model of precursor B cell acute lymphoblastic leukemia. *Proceedings of the National Academy of Sciences of the United States of America*, **103**, 15166–15171.

Santoriello, C., Gennaro, E., Anelli, V., Distel, M., Kelly, A., Köster, R.W., Hurlstone, A. & Mione, M. (2010) Kita driven expression of oncogenic HRAS leads to early onset and highly penetrant melanoma in zebrafish. *PLoS One*, **5**, e15170.

Schnell, U., Cirulli, V. & Giepmans, B.N.G. (2013) EpCAM: structure and function in health and disease. *Biochimica et Biophysica Acta*, **1828**, 1989–2001.

Shepard, J.L., Stern, H.M., Pfaff, K.L. & Amatruda, J.F. (2004) Analysis of the cell cycle in zebrafish embryos. *Methods in Cell Biology*, **76**, 109–125.

Sidi, S., Sanda, T., Kennedy, R.D., Hagen, A.T., Jette, C.A., Hoffmans, R., Pascual, J., Imamura, S., Kishi, S., Amatruda, J.F., Kanki, J.P., Green, D.R., D'Andrea, A.A. & Look, A.T. (2008) Chk1 suppresses a caspase-2 apoptotic response to DNA damage that bypasses p53, Bcl-2, and caspase-3. *Cell*, **133**, 864–877.

Swindell, W.R. (2011) Metallothionein and the biology of aging. *Ageing Research Reviews*, **10**, 132–145.

Takemoto, C.M., Lee, Y.-N., Jegga, A.G., Zablocki, D., Brandal, S., Shahlaee, A., Huang, S., Ye, Y., Gowrisankar, S., Huynh, J. & McDevitt, M.A. (2009) Mast cell transcriptional networks. *Blood Cells, Molecules & Diseases*, **41**, 82–90.

Theoharides, T.C. & Kalogeromitros, D. (2006) The critical role of mast cells in allergy and inflammation. *Annals of the New York Academy of Sciences*, **1088**, 78–99.

Traver, D., Herbomel, P., Patton, E.E., Murphey, R.D., Yoder, J.A., Litman, G.W., Catic, A., Amemiya, C.T., Zon, L.I. & Trede, N.S. (2003) The zebrafish as a model organism to study development of the immune system. *Advances in Immunology*, **81**, 253–330.

Trowbridge, J.J., Snow, J.W., Kim, J. & Orkin, S.H. (2009) DNA methyltransferase 1 is essential for and uniquely regulates hematopoietic stem and progenitor cells. *Cell Stem Cell*, **5**, 442–449.

Trowbridge, J.J., Sinha, A.U., Zhu, N., Li, M., Armstrong, S.A. & Orkin, S.H. (2012) Haploinsufficiency of Dnmt1 impairs leukemia stem cell function through derepression of bivalent chromatin domains. *Genes & Development*, **26**, 344–349.

Tsang, M. (2010) Zebrafish: a tool for chemical screens. *Birth Defects Research Part C, Embryo Today: Reviews*, **90**, 185–192.

Ustun, C., DeRemer, D.L. & Akin, C. (2011) Tyrosine kinase inhibitors in the treatment of systemic mastocytosis. *Leukemia Research*, **35**, 1143–1152.

Villablanca, E.J., Renucci, A., Sapède, D., Lec, V., Soubiran, F., Sandoval, P.C., Dambly-Chaudière, C., Ghysen, A. & Allende, M.L. (2006) Control of cell migration in the zebrafish lateral line: implication of the gene "tumour-associated calcium signal transducer", tacstd. *Developmental Dynamics: An Official Publication of the American Association of Anatomists*, **235**, 1578–1588.

Westerfield, M. (2007) The Zebrafish Book: A Guide for the Laboratory Use of Zebrafish (*Danio rerio*), 5th edn. The University of Oregon Press, Eugene, OR.

Yeh, J.-R.J., Munson, K.M., Elagib, K.E., Goldfarb, A.N., Sweetser, D.A. & Peterson, R.T. (2009) Discovering chemical modifiers of oncogene-regulated hematopoietic differentiation. *Nature Chemical Biology*, **5**, 236–243.

Yoo, S.K., Starnes, T.W., Deng, Q. & Huttenlocher, A. (2011) Lyn is a redox sensor that mediates leukocyte wound attraction in vivo. *Nature*, **480**, 109–112.

Zappulla, J.P., Dubreuil, P., Desbois, S., Létard, S., Hamouda, N.B., Daëron, M., Delsol, G., Arock, M. & Liblau, R.S. (2005) Mastocytosis in mice expressing human Kit receptor with the activating Asp816Val mutation. *The Journal of Experimental Medicine*, **202**, 1635–1641.